



## Contribution of Early-Postmortem Proteome and Metabolome to Ultimate pH and Pork Quality

Elizabeth A. Zuber<sup>1</sup>, Amanda C. Outhouse<sup>1</sup>, Emma T. Helm<sup>1</sup>, Nicholas K. Gabler<sup>1</sup>,  
Kenneth J. Prusa<sup>2</sup>, Edward M. Steadham<sup>1</sup>, Elisabeth Huff-Lonergan<sup>1</sup>, and Steven M. Lonergan<sup>1\*</sup>

<sup>1</sup>Department of Animal Science, Iowa State University, Ames, IA 50011, USA

<sup>2</sup>Department of Food Science and Human Nutrition, Iowa State University, Ames, IA 50011, USA

\*Corresponding author. Email: [slonerga@iastate.edu](mailto:slonerga@iastate.edu) (Steven M. Lonergan)

**Abstract:** This study's objectives were to identify how subtle differences in ultimate pH relate to differences in pork quality and to understand how early-postmortem glycolysis contributes to variation in ultimate pH. The hypothesis was that elements in early-postmortem *longissimus thoracis et lumborum* proteome and metabolome could be used to predict quality defects associated with pH decline. Temperature and pH of the *longissimus thoracis et lumborum* were measured at 45 min, 24 h, and 14 d postmortem. Quality measurements were made after 14 d of aging. Groups were classified as normal pH (NpH;  $\bar{x}$  = 5.59 [5.53–5.67]; NpH,  $n$  = 10) and low pH (LpH;  $\bar{x}$  = 5.42 [5.38–5.45]; LpH,  $n$  = 10) at 14 d postmortem. Metabolites from 45 min postmortem were identified using GC-MS. Relative differences between proteins were quantified with two-dimensional difference in gel electrophoreses, and spots were identified with MALDI-MS. Western blot analyses were used to measure phosphofructokinase, peroxiredoxin-2, and reduced and non-reduced adenosine monophosphate deaminase-2 at 45 min and 14 d postmortem. Ultimate pH classification did not affect 45-min-postmortem pH ( $P$  = 0.64); 14-d pH was different between groups ( $P$  < 0.01). NpH had less purge loss ( $P$  < 0.01), was darker ( $P$  < 0.01), had lower star probe ( $P$  < 0.01), and had less intact day-7 desmin ( $P$  = 0.02). More pyruvate ( $P$  = 0.01) and less lactate ( $P$  = 0.09) was observed in NpH, along with more soluble lactate dehydrogenase ( $P$  = 0.03) and pyruvate kinase ( $P$  < 0.10). These observations indicate that differences in enzyme abundance or solubility may produce more pyruvate and less lactate. Fructose 6-phosphate was more abundant ( $P$  = 0.08) in the LpH group, indicating that phosphofructokinase may be involved in glycolytic differences. Furthermore, greater abundance of heat shock proteins, peroxiredoxin-2 ( $P$  = 0.02), and malate ( $P$  = 0.01) early postmortem all suggest differences in mitochondrial function and oxidative stability that contribute to quality differences. These results show that even subtle changes in ultimate pH can influence pork quality. The proteome and metabolome at 45 min postmortem are associated with variation in the extent of pH decline.

**Key words:** pork quality, ultimate pH, glycolysis, metabolomics, proteomics

*Meat and Muscle Biology* 5(1): 13, 1–17 (2021)

doi:10.22175/mmb.11709

Submitted 24 November 2020

Accepted 26 January 2021

## Introduction

Classification of pork, based on quality, creates an opportunity for processors and producers to differentiate their products in a value-based marketing effort. Quality-based classification could allow purveyors, chefs, retailers, and consumers to make purchases that meet their expectations (Lusk et al., 2018). Factors that control meat quality characteristics include marbling, color, texture, and juiciness (Brewer et al.,

2001; Font-i-Furnols and Guerrero, 2014). The rate and extent of pH decline cause variation in those factors (Huff-Lonergan et al., 2002; England et al., 2013; Subramanian et al., 2017). Therefore, ultimate pH in the loin is a useful indicator of fresh pork quality.

Meat quality development begins with the live animal and is reliant on early-postmortem conditions. Following exsanguination, calcium accumulation and ischemia initiate skeletal muscle's attempt to maintain homeostasis. Energy metabolism, including hydrolysis

of adenosine triphosphate (ATP), enables the onset of rigor mortis. Sources of postmortem ATP production are aerobic metabolism through the citric acid cycle, fatty acid and lipid oxidation, and anaerobic metabolism through the glycolytic pathway (Westerblad et al., 2010). The demand for energy regeneration and limited oxygen in these circumstances creates a conversion from aerobic metabolism to anaerobic metabolism (Ohlendieck, 2010). Therefore, enzymes and metabolites in those pathways provide clues to explain the dynamic changes that occur in early-postmortem meat that can have profound impacts on pork quality.

Three parameters dictate the initial decline in pH (until ~5.5 pH): (1) temperature of the skeletal muscle, (2) skeletal muscle glycogen content at harvest, and (3) substrate that passes phosphofructokinase (PFK) in glycolysis (England et al., 2014). Glycogen is the substrate for glycogenolysis and glycolysis to generate ATP. Thus, the amount of glycogen directly impacts postmortem glycolytic potential (Mookerjee et al., 2016). A greater abundance of skeletal muscle glycogen at the time of harvest contributes to lower ultimate pH, but only if glycogen content is below 50 mmol glycogen/kg wet weight (Henckel et al., 2002).

Phosphofructokinase uses ATP to catalyze the conversion of fructose 6-phosphate to fructose 1,6-bisphosphate. The PFK reaction is one of the rate-limiting steps in glycolysis, the others being glycogen phosphorylase and pyruvate kinase (PK) (Scheffler and Gerrard, 2007). England et al. (2015) identified PFK to regulate the rate of pH decline *in vitro* because of the amount of substrate that passes PFK until about pH 5.5, when PFK loses activity. A fast rate of glycolysis, termed glycolytic flux, can result in a low ultimate pH, yet once the pH reaches ~5.5, the conversion of fructose 6-phosphate to fructose 1,6-bisphosphate slows. Therefore, PFK impacts pH decline by limiting the production of substrate for ATP regeneration systems (glycolysis, citric acid cycle, mitochondria and nucleotide recycling).

The complex environment in early-postmortem meat has made it difficult to determine specific metabolic events or conditions that control variation in the extent of pH decline. There is some evidence that PFK activity, adenosine monophosphate (AMP) deaminase activity, and mitochondrial stability are associated with variation in pH decline below pH 5.5 (England et al., 2014, 2015; Matarneh et al., 2017b). The establishment of these molecular factors' contribution is necessary to understand subtle changes in pH decline that result in substantial variation in quality and value.

Many studies conclude that the time to measure ultimate pH is at 24 h postmortem, assuming that the carcass has completed rigor mortis and will no longer decrease in pH (Richardson et al., 2018; Honegger et al., 2019). However, others have identified a more extended decline in pH and development of quality characteristics beyond 24 h postmortem (Tarczyński et al., 2018). Therefore, defining a connection between glycolytic flux and glycolytic capacity in early-postmortem muscle with ultimate pH will extend our understanding and control of subtle factors that affect pork quality. This is vital to detect 14-d-postmortem pork quality from early-postmortem samples, especially when the 14-d pH is <5.5.

Herein, we proposed to test 2 unique hypotheses. First, small variations in ultimate pH at 14 d postmortem will result in a significant difference in pork quality. Second, natural variations in the glycolytic capacity are related to ultimate pH and are detectable in metabolomic and proteomic profiles at 45 min postmortem. The objectives were to determine the extent to which early-postmortem proteome and metabolome are related to ultimate pH and pork loin quality.

## Materials and Methods

### Sample preparation

Fresh pork samples were obtained from 47 market weight (~125 kg) Yorkshire barrows selected from the 11th generation high and low residual feed intake (RFI) selection lines at Iowa State University and were raised and harvested according to Outhouse et al. (2019). *Longissimus thoracis et lumborum* samples were excised from the rib on the left side at 45 min postmortem. Carcasses were placed in a cooler at -2°C. The loin was removed from the right side of each carcass 1 d postmortem, cut into chops (2.54 cm thick), vacuum packaged, and aged for 1, 7, and 14 d in the dark. Vacuum packages (Cryovac, Sealed Air Corporation, Duncan, SC) consisted of an oxygen transmission rate of 1.5 to 3.5 cm<sup>3</sup>/0.06 m<sup>2</sup>/24 h/1 atmosphere at 5°C and 0% relative humidity and a water vapor transmission rate of 0.3 to 0.6 g/0.06 m<sup>2</sup>/24 h/1 atmosphere at 38°C and 100% relative humidity. Temperature and pH measurements were made on aged chops, and 14-d-postmortem pH measurements were used to sort carcasses into groups of normal (*n* = 10) and low (*n* = 10) ultimate pH categories.

## Temperature and pH

A portable Hanna I9025 pH meter (Hanna Instruments, Woonsocket, RI) was calibrated and used for pH and temperature measurements. Calibration was done using a pH 4 and pH 7 buffer to ensure that the pH remained within the range of pH 4 and  $7 \pm 0.05$ . pH was measured (in duplicate) at the 13th rib on the left side, and the temperature was measured 5 cm cranial to the point of pH measurement at each time point: 0.75, 3, 6, and 24 h. The pH was measured at day 14 on aged chops after chops were allowed to bloom for 15 min at room temperature ( $\sim 22^\circ\text{C}$ ).

Carcasses ( $n = 47$ ) were sorted according to day-14 pH, and a subsample of normal pH (NpH; pH,  $\bar{x} = 5.59$  [5.53–5.67];  $n = 10$ ) and low pH (LpH; pH,  $\bar{x} = 5.42$  [5.38–5.45];  $n = 10$ ) were selected for the current study. Normal- and low-pH carcasses were denoted as NpH and LpH, respectively. Since these samples were from a previous project (Outhouse et al., 2019), NpH and LpH were balanced by the selection line. Both high- and low-RFI carcasses were equally represented among pH treatment groups.

## Purge, cook loss, and star probe

At 1 d postmortem, chops (2.54 cm thick) were placed in a sealed Ziploc bag (S. C. Johnson & Son, Inc., Racine, WI) and stored at  $4^\circ\text{C}$  for 3 d. After 3 d, chops were removed from the bag and weighed. Chop purge was calculated by  $([\text{chop weight day 1} - \text{chop weight day 3}]/\text{chop wt. day 1}) \times 100$ . For star probe and cook loss analysis, chops were aged for 14 d. After aging, chops were removed from the bag and weighed before being allowed to bloom for  $\sim 15$  min at room temperature (approximately  $22^\circ\text{C}$ ). Visible fat was removed from each chop before being cooked to  $68^\circ\text{C}$  on clamshell grills (Cuisinart, Conair Corporation, Stamford, CT) and set aside to cool at room temperature (approximately  $22^\circ\text{C}$ ). Cooked chops were weighed immediately after cooking for cook loss using the equation  $([\text{raw weight} - \text{cook weight}]/\text{raw weight}) \times 100$  before cooling to room temperature. After cooling, an Instron (Instron, Grove City, PA) was used for mechanical tenderness measurements (Outhouse et al., 2019). A 5-prong probe pierced chops to 20% of their original height and measured the weight (kilograms) of pressure used for the compression (Schulte et al., 2019).

## Color and marbling

After 14 d of aging, chops were removed from the vacuum seal bag and allowed to bloom for 15 min.

Hunter L, a, and b color values were determined (L: lightness; a: redness; and b: yellowness) using a Hunter Minolta Colorimeter (CR-410; Konica Minolta Sensing Americas, Inc., Ramsey, NJ) with a D65 light source, 50-mm aperture, and  $0^\circ$  observer. At 14 d postmortem, marbling and color scores were assigned by Outhouse et al. (2019) using standards established by the NPPC (2000) (color: 6-point scale, 1 = pale pinkish gray to white; 6 = dark purplish red; marbling: 10-point scale, 1 = 1.0% intramuscular fat; 10 = 10.0% intramuscular fat).

## Desmin degradation

Densitometry analysis of immunoblots was used to quantify intact desmin, resolved in the whole muscle extracts from samples aged 1, 7, and 14 d. Whole muscle samples from 1, 7, and 14 d postmortem were prepared according to Outhouse et al. (2019) for sodium dodecyl sulphate–polyacrylamide gel electrophoresis (SDS-PAGE) western blotting. Rabbit anti-desmin antibody produced at Iowa State University (Carlson et al., 2017) was used for primary antibody and diluted in phosphate-buffered saline (PBS)-Tween (1:40,000). The intensity of intact (55 kDa) desmin was standardized across gel as a ratio of the immunoreactive intact desmin bands from each sample to the intensity of the immunoreactive desmin from the intact band of the internal reference sample. All samples were run in duplicate.

## Two-dimensional difference in gel electrophoresis

Samples from 45 min postmortem were snap frozen immediately after excision in liquid nitrogen, then homogenized into a powder using a Waring Blender (Waring Commercial, New Hartford, CT) and stored until further evaluation in a  $-80^\circ\text{C}$  cooler. Samples were prepared by homogenizing 3 g of muscle with 10 mL of low-ionic-strength buffer (50 mM Tris-HCl, 1 mM ethylene diamine tetraacetic acid [EDTA] [pH 8.5]) using a Polytron PT 3100 (Kinematica, Lucerne, Switzerland). Homogenized proteins were centrifuged at  $24,000 \times g$  for 20 min at  $4^\circ\text{C}$ . Samples were poured into a second tube through cheesecloth to separate the supernatant from the pellet. Protein concentrations were determined (Lowry et al., 1951) using a BioRad DC Assay kit (BioRad, Hercules, CA). Aliquots of samples were diluted to a 10 mg/mL sample protein concentration using cold low-ionic-strength buffer and frozen. Equal parts of all samples ( $n = 20$ ) were pooled into aliquots for reference samples. Protein

concentration consistencies were measured using 15% acrylamide and SDS-PAGE and then staining the gel with Colloidal Coomassie Blue stain (1.7% ammonium sulfate, 30% methanol, 3% phosphoric acid, and 0.1% Coomassie G-250).

Samples from NpH or LpH groups were organized, paired, and assigned to 1 of 10 immobilized pH gradient (IPG) strips (either pH 3–10 [18-1016-61; GE Healthcare, Piscataway, NJ] or pH 4–7 [18-1016-60; GE Healthcare]). The samples were then labeled with CyDye 3 or CyDye 5 and alternated between samples in the NpH and LpH groups. A pooled reference sample was labeled with CyDye 2 and was included on each strip. Labeled samples and references contained a protein concentration of 7.14 mg/mL and were stored at  $-80^{\circ}\text{C}$ .

### ***pH 3–10 and pH 4–7 strip rehydration***

Similar procedures for isoelectric focusing (pH 3–10 and pH 4–7) were used. All gels were run in duplicate. Labeled samples (30  $\mu\text{g}$  of the reference, NpH, and LpH each) were combined (CyDye 2 reference, with CyDye 3 and CyDye 5 labeled samples; 90  $\mu\text{g}$  total). Combined samples were added to rehydration solution (DeStreak, GE Healthcare) containing 1.5% IPG buffer (pH 3–10 or pH 4–7; GE Healthcare) and 20 mM 1,4-dithiothreitol (DTT) and mixed. This solution was applied to 11-cm IPG strips (pH 3–10 or 4–7; GE Healthcare) in individual wells of a humidified rehydration chamber. The strips were rehydrated (15 h) in the dark at room temperature ( $\sim 24^{\circ}\text{C}$ ).

### ***Two-dimensional difference in gel electrophoresis***

The first dimension focusing was achieved with an Ettan IPGphor isoelectric focusing system (GE Healthcare) using 11,500 volt-h (pH 3–10) or 14,000 volt-h (pH 4–7). Strips were incubated (15 min) in equilibration buffer (50 mM Tris-HCl [pH 8.8], 6 M urea, 30% glycerol, 2% SDS, and trace amounts of bromophenol blue) with 67 mM DTT. A second incubation (15 min) was in equilibration buffer with 135 mM iodoacetamide. Proteins were fractionated on 12.5% polyacrylamide gels (25.5  $\times$  20.5 cm, 1.5 mm thick; acrylamide: N,N'-bis-methylene acrylamide = 100:1 [wt/wt], 0.1% [wt/vol] SDS, 0.05% [vol/vol] tetramethylene diamine, 0.05% [wt/vol] ammonium persulfate, 0.5 M Tris-HCl [pH 8.8]) using an Ettan DALT SIX system (GE Healthcare Piscataway, NJ). Gels were run (approximately 2,500 volt-h) with a buffer containing 25 mM Tris, 192 mM glycine, 2 mM EDTA, and 0.1% [wt/vol]

SDS. Gels were imaged using an Ettan DIGE Imager (GE Healthcare). Protein abundance differences between groups were identified using Melanie 9 software (Cytiva, Marlborough, MA).

### ***Spot identification***

Spots identified to be different between experimental groups ( $P < 0.10$ ) were chosen for identification (Figure 1). A pooled reference sample was used for protein spot identification. SDS-PAGE gels (12.5%) were run as described with the pH 3–10 or 4–7 range with slight modification (1.15 mg of protein was added to rehydration solution [DeStreak, GE Healthcare] and prepared according to the manufacturer's instructions by combining 2% IPG buffer and 20 mM DTT) to isolate spots of interest.

Gel slices were sent to the Iowa State University Protein Facility and digested with 1  $\mu\text{g}$  of trypsin for 10 h on the Investigator ProGest (Genomic Solutions) automated digester. The peptides were then separated by liquid chromatography (Thermo Scientific EASY nLC-1200 coupled to a Thermo Scientific Nanospray FlexIon source) and analyzed by MS/MS on a Thermo Scientific Q Exactive Hybrid Quadrupole-Orbitrap Mass Spectrometer (Schulte et al., 2020). Raw data are analyzed using Thermo Scientific's Proteome Discoverer Software, version 2.4.0.305. The data were searched using Mascot version 2.2.7 and Sequest HT Uniprot-Sus scrofa on March 20, 2020, to identify proteins. Identification used a target false discovery rate of 0.05.

### ***Western blotting***

Sarcoplasmic protein extractions were performed as described previously using cold sarcoplasmic extraction buffer (50 mM Tris-HCl, 1 mM EDTA [pH 8.5]). Protein concentration was adjusted to 4 mg protein/mL in each sample using low-ionic-strength extraction buffer, 500  $\mu\text{L}$  of Wangs tracking dye (3 mM EDTA, 3% [wt/vol] SDS, 30% [vol/vol] glycerol, 0.01% [wt/vol] pyronin-Y, 30 mM Tris-HCl [pH 8.0]), and 100  $\mu\text{L}$  of mercaptoethanol (reduced samples) or 100 additional  $\mu\text{L}$  of tracking dye (non-reduced samples). All prepared samples were vortexed, and then reduced samples were heated to  $50^{\circ}\text{C}$  for 20 min. Non-reduced samples were not heated. All samples were stored at  $-80^{\circ}\text{C}$  until further use.

Polyacrylamide separating gels and stacking gels were made according to Carlson et al. (2017). Acrylamide percentages for each gel were dependent upon target antibody; peroxiredoxin-2 (10%), AMP deaminase-2

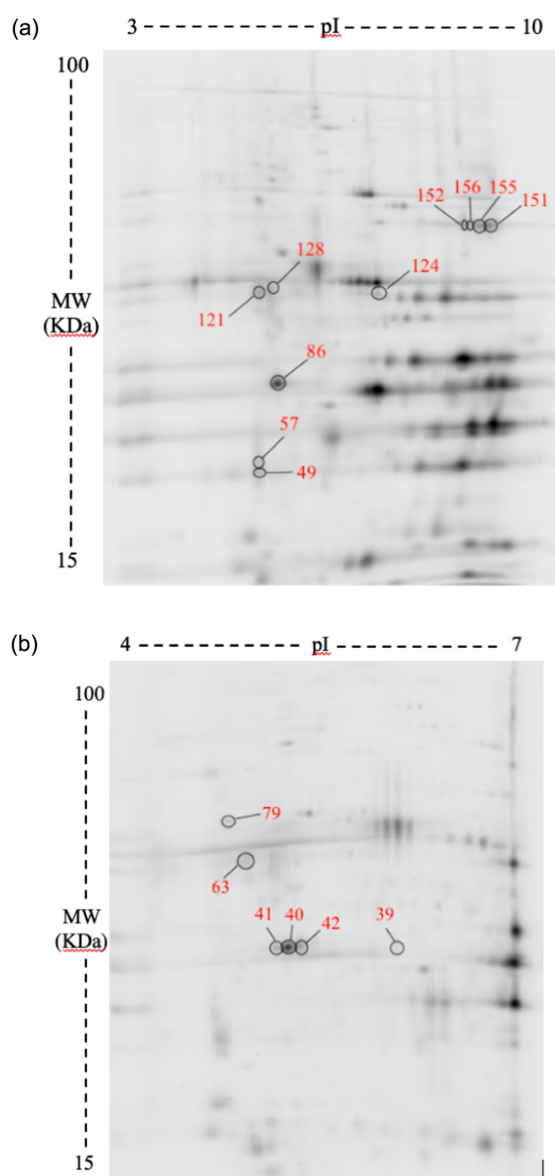


**Figure 1.** Spot identification of two-dimensional difference in gel electrophoreses from the sarcoplasmic fraction of 45-min–postmortem pork *longissimus thoracis et lumborum* between day 14 postmortem pH classified as normal pH (pH,  $\mu = 5.59$  [5.53–5.67]) and low pH (pH,  $\mu = 5.42$  [5.38–5.45]). Spots correspond to numbers in image (A) immobilized pH gradient (IPG) strip pH 3–10 and (B) IPG strip pH 4–7. Fructose biphosphate aldolase (Spot 152, 156, 155, 151), pyruvate kinase (Spot 124, 121, 63),  $\alpha$ 2-heat shock glycoprotein (Spot 128), glyceraldehyde 3-phosphate dehydrogenase (Spot 57), L-lactate dehydrogenase (Spot 49), heat shock protein 70 (Spot 79),  $\beta$ -enolase (Spot 39), and  $\alpha$ -actin (Spot 86, 41, 40, 42). CyDye labeled protein was loaded onto the 11-cm IPG strips and run on a 12.5% sodium dodecyl sulphate–polyacrylamide gel electrophoresis gel. Proteins in this image are labeled with Cy5.

reduced (15%), AMP deaminase-2 non-reduced (8%), and PFK (15%). Day 0 (45 min), reduced and non-reduced reference samples were prepared by pooling equal parts from all 45-min gel samples.

Gel samples and their references (40  $\mu$ g of protein) were resolved in SE 260 Hoefer Mighty Small II electrophoresis units (Hoefer, Inc., Holliston, MA)

and transferred using a TE-22 Mighty Small Transfer unit (Hoefer, Inc.) combined with transfer buffer (25 mM Tris, 192 mM glycine, 2 mM EDTA, and 15% [vol/vol] methanol) (Carlson et al., 2017) onto polyvinylidene difluoride membranes with pore sizes of 0.2  $\mu$ m. Membranes were incubated with primary antibodies diluted in PBS-Tween (peroxiredoxin-2: 1:20,000, rabbit, monoclonal, Ab109367, Abcam [Cambridge, MA]; PFK: 1:40,000, rabbit, monoclonal, Ab154804, Abcam; AMP deaminase-2: 1:5,000, mouse, monoclonal, Sc-100504, Santa Cruz Biotechnology [Dallas, TX]) (~15 to 20 h) at 4°C. Membranes were incubated with secondary antibodies diluted in PBS-Tween (goat anti-rabbit IgG [HRP]: 1:10,000, 31460, Thermo Fisher Scientific [Rockford, IL]; goat anti-mouse IgG [HRP]: 1:10,000, A2554, Sigma-Aldrich [St. Louis, MO]) for 1 h at room temperature (~22°C). Membranes were washed for three 10-min intervals with PBS-Tween. A chemiluminescent detection kit (ECL Prime, GE Healthcare) was used to detect proteins. Densitometry of proteins was analyzed using a ChemiImager 5500 (Alpha Innotech, San Leandro, CA) and Alpha Ease FC software (version 4.0; Alpha Innotech). Phosphofructokinase, reduced AMP deaminase-2, and peroxiredoxin-2 densitometry results were analyzed as a ratio of the sample immunoreactive band's intensity to the internal reference immunoreactive band. Non-reduced AMP deaminase-2 was analyzed as a ratio of the intensity of the sample's immunoreactive band to its respective immunoreactive band in the internal reference. Western blots were completed in duplicate.

### Nontargeted metabolomics

Total metabolite analysis was conducted at the W. M. Keck Metabolomics Research Laboratory (Ames, IA) using an Agilent Technologies model 6890 gas chromatograph coupled to a model 5973 mass selective detector (GC-MS) (Agilent Technologies, Santa Clara, CA). Ribitol and nonadecanoic fatty acid (10  $\mu$ L, 1.5 mg/mL) were added to 100 mg of frozen (at  $-80^{\circ}$ C) and pulverized muscle samples. All preparation steps were conducted on ice. Methanol was added (ice-cold high performance liquid chromatography grade; 500  $\mu$ L) to the samples, which were then sonicated (in an ice-cold water bath for 10 min), vortexed, and centrifuged (at  $16,300 \times g$  for 7 min at  $\sim 22^{\circ}$ C). Chloroform was added (400  $\mu$ L), and samples were vortexed before adding 0.34 mL of high performance liquid chromatography grade water. Samples were vortexed, sonicated (in an ice-cold water bath for 10 min),

and centrifuged (at  $16,000 \times g$  for 7 min at  $\sim 22^\circ\text{C}$ ). The polar top and nonpolar bottom portions were transferred to a GC vial for GC-MS derivatization.

Extracts were dried using a speed vac overnight ( $\sim 15$  h). After drying, samples were derivatized by adding 50  $\mu\text{L}$  of freshly prepared methoxyamine hydrochloride (20 mg/mL in pyridine) and incubated at  $30^\circ\text{C}$  for 90 min. Bis-trimethyl silyl trifluoroacetamide (70  $\mu\text{L}$ ) with 1% trimethylchlorosilane was added for silylation and incubated at  $60^\circ\text{C}$  for 30 min.

Samples were run on the same instrument (Agilent Technologies Model 6890 GC coupled to Model 5975 MS), and a hydrocarbon ladder was used as a retention index calibrator. Sample separation was completed on a GC-MS column (Agilent-HP5MSI;  $30\text{ m} \times 250\ \mu\text{M} \times 0.25\ \mu\text{M}$ ). The oven program used an initial temperature of  $70^\circ\text{C}$  for 0.5 min, a  $10^\circ\text{C}/\text{min}$  ramp to  $160^\circ\text{C}$ , and a  $5.5^\circ\text{C}/\text{min}$  ramp to  $320^\circ\text{C}$  with a final hold for 6.4 min. Inlet and interface temperatures were controlled at  $280^\circ\text{C}$ .

The detection mass range was set to 40–600 m/z. The Agilent ChemStation software controlled the GC-MS. The National Institutes of Standards and Technology mass spectral library (NIST, 2017) served as references for metabolites identified using the total ion mass spectrum. The amount of ribitol (0.0098  $\mu\text{mol}$ ) and nonadecanoic acid (0.005  $\mu\text{mol}$ ) added to each sample was used to normalize and quantify MS peak areas for each polar and nonpolar metabolite, respectively.

### Statistical analysis

Statistical analysis for pH, temperature, and quality (purge, cook loss, star probe, color, marbling, and intact desmin) was done with mixed procedures of SAS version 9.4 (SAS Institute Inc., Cary, NC) and the fixed effect of 14-d pH classification. Line (RFI) was included as a fixed effect and removed from the model when there was no statistical significance ( $P > 0.05$ ). Phosphofructokinase, AMP deaminase-2 (reduced and non-reduced), and peroxiredoxin-2 were analyzed using the mixed procedure of SAS version 9.4 with fixed effects of 14-d pH classification (NpH or LpH), time postmortem (45 min or 14 d), and their interaction. Gel was used as a random effect in the model. Statistical significances ( $P < 0.05$ ) or trends ( $P < 0.10$ ) were reported for pH classification and time postmortem.

The Statistical Analysis module of MetaboAnalyst 4.0 (Chong et al., 2018) was employed to analyze metabolite results. Metabolites that contained  $>80\%$

missing values were removed from the dataset. The K-nearest neighbor method was used to replace missing values for metabolites that were not removed. The identified glycolytic metabolites were analyzed using a Student  $t$  test, and differential abundance between NpH and LpH was reported as fold changes (fold change =  $\text{NpH}/\text{LpH}$ ;  $P < 0.1$ ). Results from two-dimensional difference in gel electrophoreses were analyzed through Melanie 9 (Cytiva) using a paired  $t$  test. Differential abundance between NpH and LpH were reported as fold changes (fold change =  $\text{NpH}/\text{LpH}$ ;  $P < 0.15$ ).

## Results

### Meat quality, temperature, and pH decline

Day-14 pH differed between classification groups (NpH,  $\bar{x} = 5.59$  [5.53–5.67]; LpH,  $\bar{x} = 5.42$  [5.38–5.45]). Day-14 pH did not affect 45-min pH and only tended to affect 24-h pH ( $P = 0.10$ ; Table 1). Normal-pH chops had lower star probe values ( $P < 0.05$ ). Normal-pH chops were darker, with lower Hunter L values ( $P < 0.05$ ). Less purge loss ( $P < 0.05$ ) and less cook loss ( $P < 0.05$ ) was observed in the NpH group compared with the LpH group (Table 2). These results were consistent with the observation of less intact desmin at day 7 ( $P < 0.05$ ) and a tendency for less intact desmin at day 14 ( $P < 0.10$ ) postmortem in the NpH group compared with the LpH group. The temperature at 45 min, 3 h, 6 h, and 24 h was not different between classifications ( $P > 0.10$ ; Table 1). Ultimate pH classification did not affect marbling or Hunter a value ( $P > 0.10$ ; Table 2).

**Table 1.** Summary of pork *longissimus thoracis et lumborum* pH and temperature ( $^\circ\text{C}$ ) measurements between day-14–postmortem pH classified as NpH (pH,  $\bar{x} = 5.59$  [5.53–5.67]) and LpH (pH,  $\bar{x} = 5.42$  [5.38–5.45])

	NpH (n = 10)	LpH (n = 10)	P Value	SEM
45-min pH	6.39	6.44	0.64	0.06
3-h pH	5.99	5.91	0.48	0.08
6-h pH	5.78	5.69	0.38	0.07
24-h pH	5.62	5.56	0.08	0.02
14-d pH	5.59	5.42	$<0.01$	0.01
45-min temperature	40.0	39.1	0.17	0.4
3-h temperature	23.8	24.8	0.29	0.7
6-h temperature	11.7	12.4	0.32	0.5
24-h temperature	0.0	0.0	0.32	0.02

LpH = low pH; NpH = normal pH; SEM = standard error of the mean.

**Table 2.** Summary of pork *longissimus thoracis et lumborum* quality measurements between day-14–postmortem pH classified as NpH (pH,  $\bar{x}$  = 5.59 [5.53–5.67]) and LpH (pH,  $\bar{x}$  = 5.42 [5.38–5.45])

	NpH (n = 10)	LpH (n = 10)	P Value	SEM
Star Probe (kg) <sup>1</sup>	5.36	6.41	<0.01	0.20
Average Chop Purge % <sup>2</sup>	2.40	3.84	<0.01	0.32
Cook Loss % <sup>3</sup>	20.21	22.81	0.03	0.77
Color Score <sup>4</sup>	3.2	2.8	0.06	0.16
Hunter L	47.63	50.59	<0.01	0.67
Hunter a	15.03	15.06	0.92	0.27
Hunter b	6.74	7.58	0.02	0.23
Marbling <sup>5</sup>	2.1	2.0	0.66	0.24
Intact Desmin Intensity <sup>6</sup>				
Day 1 postmortem	4.11	4.72	0.28	0.38
Day 7 postmortem	1.78	3.39	0.02	0.45
Day 14 postmortem	1.43	2.36	0.06	0.33
Myosin Heavy Chain IIb (%) <sup>7</sup>	77.9	79.6	0.84	5.8
Myosin Heavy Chain IIa + IIx (%) <sup>7</sup>	22.1	19.9	0.78	5.8

Subjective color and marbling, cook loss, and star probe were evaluated on chops aged 14 d.

<sup>1</sup>Force utilized to compress the sample to 20% of its original height.

<sup>2</sup>Purge loss % = [(initial weight (day 1) – final weight (day 3))/initial weight] × 100.

<sup>3</sup>Cooked to an internal temperature of 68°C; cook loss % = [(raw weight – cooked weight)/raw weight] × 100.

<sup>4</sup>National Pork Board standards, 6-point scale (1 = pale pinkish gray to white; 6 = dark purplish red).

<sup>5</sup>National Pork Board standards, 10-point scale (1 = 1.0% intramuscular fat; 10 = 10.0% intramuscular fat).

<sup>6</sup>55 kDa intact immunoreactive band was measured as a ratio to the intensity of the immunoreactive desmin from the intact band of the internal reference sample.

<sup>7</sup>Proportion of myosin heavy chain detected as type IIa + IIx or IIb based on SDS-PAGE migration. Protein samples prepared from *longissimus dorsi* muscle removed from the carcass at 45 min postmortem (Carlson et al., 2017).

LpH = low pH; NpH = normal pH; SDS-PAGE = sodium dodecyl sulphate–polyacrylamide gel electrophoresis; SEM = standard error of the mean.

### Glycolytic metabolite abundance

The focus of this study was on early-postmortem energy metabolism. Therefore, the metabolites of interest were those involved in glycolysis or the citric acid cycle. Metabolomic analysis of 45-min–postmortem samples identified 11 metabolites involved in glycolysis or the citric acid cycle (Table 3). Pyruvate ( $P = 0.01$ ) and malate ( $P < 0.01$ ) were both in greater abundance in the NpH group ( $P < 0.01$ ). Fructose 6-phosphate ( $P = 0.06$ ) and lactate ( $P = 0.09$ ) tended to be greater in the LpH group. Additional significant ( $P < 0.10$ ) polar and nonpolar metabolites are included in the supporting information found in Supplemental Table 1.

**Table 3.** Nontargeted analysis of glycolytic and citric acid cycle metabolites identified in 45-min–postmortem pork *longissimus thoracis et lumborum* samples

Pathway	Metabolite	Fold Change	P Value
Glycolysis	Glucose	0.90	0.67
	Glucose 6-phosphate	1.42	0.23
	Fructose 6-phosphate	0.78	0.08
	Fructose 1,6-bisphosphate	1.45	0.52
	Glycerate 3-phosphate	1.39	0.11
	Lactate	0.59	0.09
Citric Acid Cycle	Pyruvate	1.98	0.01
	Citrate	1.19	0.58
	Succinate	1.08	0.72
	Fumarate	1.34	0.19
	Malate	1.59	0.01

Classification was between day-14–postmortem pH classified as NpH (pH,  $\bar{x}$  = 5.59 [5.53–5.67]) and LpH (pH,  $\bar{x}$  = 5.42 [5.38–5.45]). Fold change is shown as NpH/LpH.

LpH = low pH; NpH = normal pH.

### Sarcoplasmic protein abundance

Analysis of two-dimensional difference in gel electrophoresis resulted in 117 spots for the pH 4–7 and 89 spots in the pH 3–10. Of those, 11 total spots were selected for proteomic identification. Proteins of interest (8 proteins) were all higher in the NpH group compared with the LpH group (Table 4). Differentially abundant proteins were involved in glycolysis (fructose bisphosphate aldolase [ALDO], PK, glyceraldehyde 3-phosphate dehydrogenase [GAPDH],  $\beta$ -enolase, and L-lactate dehydrogenase [L-LDH]), muscle contraction ( $\alpha$ -actin), or heat shock regulation ( $\alpha$  2-heat shock glycoprotein and heat shock protein 70 [HSP70]).

### Western blot analysis

Peroxioredoxin-2 was significantly higher in the NpH group than the LpH group at 45 min postmortem ( $P = 0.02$ ), but no difference was detected at 14 d postmortem ( $P > 0.10$ ) (Table 5). Regardless of pH classification, PFK decreased from 45 min to 14 d postmortem ( $P < 0.01$ ). Adenosine monophosphate deaminase-2 was evaluated on nonreducing gels and revealed 4 immunoreactive bands that were analyzed at 45 min postmortem (Figure 2). However, no significant differences were detected between ultimate pH groups ( $P > 0.10$ ; Figure 2). Reduced AMP deaminase-2 was greater at 45 min postmortem ( $P < 0.01$ ) compared with 14 d postmortem (Table 6; Figure 3) when NpH and LpH groups were combined.

**Table 4.** Proteomic analysis of the differentially abundant proteins from the sarcoplasmic fraction in 45-min–postmortem pork *longissimus thoracis et lumborum* samples

	Spot ID	Spot #	Fold Change	P Value
Glycolysis	ALDO	152 <sup>1</sup>	1.25	0.04
	ALDO	156 <sup>1</sup>	1.29	0.07
	ALDO	155 <sup>1</sup>	1.30	0.07
	ALDO	151 <sup>1</sup>	1.27	0.09
	PK	124 <sup>1</sup>	1.25	0.05
	PK	121 <sup>1</sup>	1.15	0.10
	PK	63 <sup>2</sup>	1.52	0.08
	GAPDH	57 <sup>1</sup>	1.49	0.02
	β-enolase	39 <sup>2</sup>	1.50	0.08
	L-LDH	49 <sup>1</sup>	1.56	0.03
Heat Stress	HSP70	79 <sup>1</sup>	1.44	0.13
	α 2-heat shock glycoprotein	128 <sup>1</sup>	1.33	0.06
Contraction	α-actin	86 <sup>1</sup>	1.93	0.01
	α-actin	41 <sup>2</sup>	2.07	0.04
	α-actin	40 <sup>2</sup>	2.32	0.04
	α-actin	42 <sup>2</sup>	1.76	0.06

Classifications on day-14 pH were NpH (pH,  $\bar{x}$  = 5.59 [5.53–5.67]) and LpH (pH,  $\bar{x}$  = 5.42 [5.38–5.45]). Fold change is shown as NpH/LpH.

<sup>1</sup>Immobilized pH gradient strip, pH 3–10.

<sup>2</sup>Immobilized pH gradient strip, pH 4–7.

ALDO = fructose biphosphate aldolase; GAPDH = glyceraldehyde 3-phosphate dehydrogenase; HSP70 = heat shock protein 70; L-LDH = L-lactate dehydrogenase; LpH = low pH; NpH = normal pH; PK = pyruvate kinase.

Ultimate pH classification had no effect on the abundance of PFK at 45 min ( $P > 0.10$ ) or 14 d ( $P > 0.10$ ) postmortem between NpH and LpH groups (Table 5). Reduced AMP deaminase-2 was not different at 45 min ( $P > 0.10$ ) or 14 d ( $P > 0.10$ ) postmortem (Table 5). The interaction of ultimate pH group by time postmortem was not significant for peroxiredoxin-1 AMP deaminase-2 or PFK. Combined NpH and LpH peroxiredoxin-2 resulted in no difference between 45 min and 14 d postmortem ( $P > 0.15$ ) (Table 6; Figure 3).

## Discussion

Glycolysis requires metabolic enzymes to yield energy from free glucose or glucose 6-phosphate. However, skeletal muscle cannot store free glucose, so it is limited in the early-postmortem environment (Kastenschmidt et al., 1968). Glucose must instead be stored as glycogen or glucose 1-phosphate. In glycogenolysis, glucose 1-phosphate is generated from removing one glucose moiety from glycogen by

**Table 5.** Western blot analysis of PFK, peroxiredoxin-2, and AMP deaminase-2 in pork *longissimus thoracis et lumborum* between day-14–postmortem pH groups, classified as NpH (pH,  $\bar{x}$  = 5.59 [5.53–5.67]) and LpH (pH,  $\bar{x}$  = 5.42 [5.38–5.45])

	NpH (n = 10)	LpH (n = 10)	P Value	SEM
PFK				
45 min, 23 kDa band	0.94	0.97	0.65	0.05
14 d, 23 kDa band	0.75	0.63	0.29	0.07
Peroxiredoxin-2				
45 min, 22 kDa band	1.20	0.83	0.02	0.10
14 d, 22 kDa band	1.15	1.29	0.63	0.21
AMP Deaminase-2				
45 min, 70 kDa band	1.08	0.84	0.36	0.18
14 d, 70 kDa band	1.63	1.33	0.46	0.27

The analysis was from 45-min–postmortem and 14-d–postmortem pork *thoracis et lumborum* sarcoplasmic samples run on SDS-PAGE gels. Samples were measured using densitometry. Effect of pH classification was measured on PFK, peroxiredoxin-2, and AMP deaminase-2 as the band area normalized as a ratio to an internal reference sample (made by pooling 45-min–postmortem sarcoplasmic samples).

AMP = adenosine monophosphate; LpH = low pH; NpH = normal pH; PFK = phosphofructokinase; SDS-PAGE = sodium dodecyl sulphate–polyacrylamide gel electrophoresis; SEM = standard error of the mean.

(a)

Non-reduced AMP Deaminase-2 Bands	Normal pH (n=10)	Low pH (n=10)	P-Value	SEM
Band 1	0.87	0.62	0.37	0.20
Band 2	1.14	1.04	0.81	0.29
Band 3	0.83	0.73	0.51	0.11
Band 4	0.83	0.73	0.84	0.17

(b) Representative western blot of non-reduced AMP deaminase-2

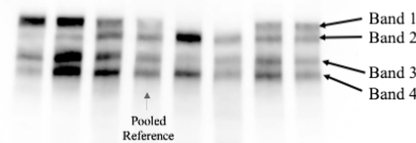


**Figure 2.** Western blot analysis of 45-min–postmortem non-reduced adenosine monophosphate (AMP) deaminase-2 between day 14 post-mortem pH classified as normal pH (pH,  $\bar{x}$  = 5.59 [5.53–5.67]) and low pH (pH,  $\bar{x}$  = 5.42 [5.38–5.45]) of non-reduced AMP deaminase-2. (A) Non-reduced AMP deaminase-2 bands were quantified as the band density ratio to its corresponding band in the internal reference sample (pooled 45-min–postmortem sarcoplasmic reference). (B) Representative western blot of non-reduced AMP deaminase-2. SEM, standard error of the mean.

**Table 6.** Effect of time analysis of PFK, peroxiredoxin-2, and AMP deaminase-2 at 45 min and 14 d postmortem using combined (NpH with LpH) mean pork *longissimus thoracis et lumborum* sarcoplasmic samples run on SDS-PAGE gels

	45 min Postmortem	14 d Postmortem	P Value	SEM
Phosphofructokinase				
23 kDa band	0.95	0.69	<0.01	0.05
Peroxiredoxin-2				
22 kDa band	1.01	1.22	0.24	0.12
AMP Deaminase-2				
70 kDa band	0.95	1.48	0.03	0.16

Samples were measured using densitometry. Bands were measured as a ratio to an internal reference sample (made by pooling 45-min–postmortem sarcoplasmic samples).

AMP = adenosine monophosphate; LpH = low pH; NpH = normal pH; PFK = phosphofructokinase; SDS-PAGE = sodium dodecyl sulphate–polyacrylamide gel electrophoresis; SEM = standard error of the mean.

glycogen phosphorylase. Glucose 1-phosphate is then isomerized to glucose 6-phosphate, which is further metabolized through glycolysis. Each glucose molecule of glycogen is converted to ATP, nicotinamide adenine dinucleotide (NADH), pyruvate, H<sup>+</sup>, and H<sub>2</sub>O in the sarcoplasm. Aerobic metabolism then converts pyruvate to ATP and H<sup>+</sup> through oxidative phosphorylation in skeletal muscle mitochondria with the citric acid cycle and the electron transport chain (Matarneh et al., 2017a). The citric acid cycle will also produce NADH and flavin adenine dinucleotide. However, limited oxygen slows aerobic metabolism, thus forcing pyruvate, NADH, and H<sup>+</sup> to be instead converted to lactate and NAD<sup>+</sup> (Matarneh et al., 2017a). These processes are essential to understand when outlining the role of metabolism in postmortem pH decline because of the substantial influence of pH on quality development in pork.

### Water-holding capacity, tenderness, and color dependence on ultimate pH

Postmortem pH decline influences the quality of fresh pork. For example, Subramaniyan et al. (2017) identified improved color scores, lightness, yellowness, drip loss, and shear force in high 24-h pH (pH 5.96) when compared to LpH (pH 5.61) pork *longissimus thoracis et lumborum*. Likewise, in the current study, the identified fresh pork quality was better in the NpH group compared with the LpH group, demonstrating that the subtle but still higher day-14 pH of the NpH group resulted in higher water-holding capacity (WHC; purge loss and cook loss), better color (color

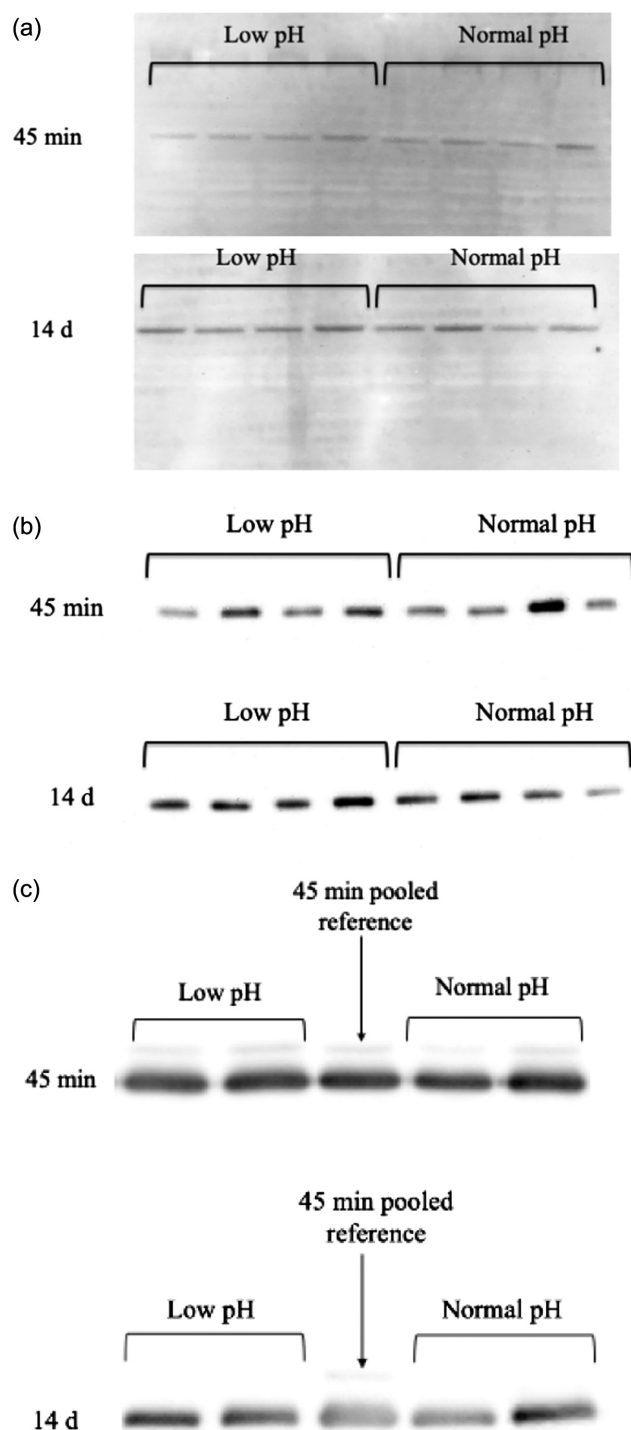


**Figure 3.** Reduced adenosine monophosphate (AMP) deaminase-2 (70 kDa), peroxiredoxin-2 (22 kDa), and phosphofructokinase (PFK) (23 kDa) bands were quantified by measuring the densitometry (area) as a ratio to the band of the internal reference sample (made by pooling 45-min–postmortem sarcoplasmic samples). Reduced (A) AMP deaminase-2, (B) peroxiredoxin-2, and (C) PFK were analyzed in 45-min–postmortem and 14-d–postmortem samples. Classification of samples was on day 14 postmortem pH as normal pH (pH,  $\bar{x}$  = 5.59 [5.53–5.67]) and low pH (pH,  $\bar{x}$  = 5.42 [5.38–5.45]).

score, lightness, yellowness), and lower star probe values. Richardson et al. (2018) argue that pH at 24 h postmortem does not influence the sensory characteristics of chops cooked to a high-endpoint cooking temperature (71°C). However, the current study shows that day-14 pH measurements (cooked to 68°C) relate to differences in quality characteristics that may not have been identifiable at 24 h postmortem.

Degradation of intermediate proteins typically indicates skeletal muscle structure changes that result in improved meat quality (Huff-Lonergan and Lonergan, 2005; Bee et al., 2007). In support of this observation, we reported greater abundance of intact desmin in the LpH group. Moreover, NpH at 14 d postmortem improves conditions for more protein degradation. More proteolysis due to higher pH at 24 h and 14 d postmortem is shown by more desmin degradation at 7 and 14 d postmortem. There was no observed difference in intact desmin at 24 h, yet pH tended to be higher in the NpH group at that time. At day 7, there was less intact desmin in the NpH group, and intact desmin still tended to be lower at day 14. These observations may be because calpain activity is pH dependent (Bee et al., 2007). Notably, calpain-1 activity is greater at higher pH (>6.5; Maddock Carlin et al., 2006). The calpains may have been more active in the NpH group at ~24 h postmortem, resulting in differences in desmin degradation at day 7 and day 14.

Peroxiredoxin-2 observed at 45 min postmortem in the current study may have contributed to quality variations between the NpH and LpH groups. Several studies have identified a greater abundance of peroxiredoxin-2 in the sarcoplasm of tough pork after 8-d aging (Carlson et al., 2017; Schulte et al., 2020). Active peroxiredoxin can inhibit oxidative stress by eliminating peroxides that increase protein oxidation (Joseph et al., 2012); therefore, it is thought to increase in response to oxidative stress. Peroxiredoxin-2, which was more abundant in high star probe classifications, has been attributed to antemortem oxidative stress that negatively impacted proteolytic mechanisms (Carlson et al., 2017; Schulte et al., 2020). However, peroxiredoxin-2 was more abundant in the current study at 45 min postmortem in the NpH group, with no differences at 14 d postmortem. Peroxiredoxin-2 may have reduced oxidation in the early-postmortem environment and protected cellular enzymes such as calpain, as some have shown that calpain activity will decrease with more oxidation (Maddock Carlin et al., 2006).

Additionally, more HSP70 and  $\alpha$  2-heat shock glycoprotein identified in the NpH group's sarcoplasm at 45 min postmortem may support proteolysis later

postmortem. Some have identified that heat shock proteins could be used as biomarkers for tenderness (Picard and Gagaoua, 2020). These proteins may prevent protein aggregates that decrease proteolysis, leading to a more tender product (Morzel et al., 2006). Yet Lomiwes et al. (2014) showed that small heat shock proteins decreased calpain activity. Furthermore, Picard et al. (2014) found HSP70 to be a useful biomarker for decreased beef tenderness. Nevertheless, this may indicate that heat shock proteins at 45 min postmortem may protect cellular functions and structures in the current study. These factors could, therefore, contribute to more desmin degradation of the NpH group.

The observed improved color and WHC in the NpH group could be due to retained water-soluble, sarcoplasmic fluid at 14 d postmortem (Mancini and Hunt, 2005; Schiaffino and Reggiani, 1996). The increased volume could allow space for fluid to be held in the resolution of rigor (Hughes et al., 2014). Sarcoplasmic proteins will precipitate at a lower pH, closer to the isoelectric point of major muscle proteins such as myosin (pI = 5.4) (Huff-Lonergan and Lonergan, 2005). When pH is near the isoelectric point, positive and negative charges are nearly equal. Therefore, protein denaturation in the LpH group may have caused myofibrillar structures to collapse, reducing cellular volume for water and water-soluble proteins, like myoglobin, to be held. Increased cellular volume resulting from protein degradation results in the improved tenderness and WHC observed in the NpH group of this study. Further investigation into the abundance of calpain and its endogenous inhibitor, calpastatin, may support the hypothesis that proteolysis allows extra myofibrillar space to hold sarcoplasmic fluid that can increase juiciness, tenderness, and color of the NpH products.

Peroxiredoxin-2 abundance at 45 min postmortem could be associated with fresh pork color at 14 d postmortem. The current study showed a greater abundance of early-postmortem peroxiredoxin-2 in the NpH group. This antioxidant protein may have contributed to early-postmortem oxidative stability and improved color in the NpH group. Joseph et al. (2012) have shown that peroxiredoxin-2 is associated with improved color stability. This could be related to the higher color scores and darker chops observed in the current study. However, color stability was not measured.

### ***Energy metabolism relationship with pH decline***

The sarcoplasmic proteome of early-postmortem meat can influence the metabolism and progression

toward the onset and completion of rigor. These factors can contribute to the variation of fresh pork quality. Glycolysis, the citric acid cycle, and postmortem temperature decline play a significant role in postmortem pH decline in meat. Unsurprisingly, several proteins of these pathways differed between the 2 pH groups.

Differences in abundance and activity of metabolic enzymes are related to postmortem muscle metabolism (England et al., 2014, 2015). Limited differences in the current study show that subtle variation in ultimate pH may not rely on enzyme abundance but rely on activity. However, further analysis of enzyme activity is necessary. Non-reduced AMP deaminase-2 results in 4 distinct bands with considerable variation in band abundances. The hypothesis was that the 4 bands in the non-reduced gels are the 4 subunits of 45-min-postmortem AMP deaminase-2 and could be used to identify differences in postmortem metabolism. If non-reduced AMP deaminase-2 was crosslinked with arbitrary proteins in the sample, the proteins would not have migrated to 4 distinct molecular weights. Therefore, these bands may indicate some biological significance in relation to the abundances of the 4 AMP deaminase-2 subunits. However, no differences were detected in the current analysis of band abundance between NpH and LpH groups. Yet there was a large amount of variation that may have shown significance with more samples. Analysis of protein abundance from 45 min to 14 d postmortem did show the combined average of both pH groups to have reduced AMP deaminase-2 and increased PFK abundance. This is potentially a result of changes in protein expression or degradation (Lametsch et al., 2003; Huff-Lonergan et al., 2010).

Pyruvate kinase catalyzes the conversion of phosphoenolpyruvate and adenosine diphosphate to pyruvate and ATP. This enzyme is an essential rate-limiting enzyme of glycolysis (Matarneh et al., 2017b). Pyruvate kinase is related to quality development because its tolerance of pH decline can vary with post-translational modifications (Schwägele et al., 1996). For example, a more rapid rate of pH decline (as defined by pH at 3 h postmortem) was associated with phosphorylation of PK, indicating a greater rate of activity (Huang et al., 2011). That study showed that rate of pH decline classification did not affect ultimate pH. Similarly, nitrosylation may influence postmortem PK activity. Pyruvate kinase activity was greater at 1 h postmortem in pale soft and exudative pork than red firm and nonexudative pork, potentially because of greater nitrosylation levels of the red firm and non-exudative pork (Wang et al., 2020). Therefore, more

phosphorylation and less nitrosylation are observed in pale soft and exudative pork because it may increase the enzyme's activity and extend postmortem glycolysis (Schwägele et al., 1996; Wang et al., 2020). In the current study, a greater abundance of PK at 45 min was observed in conjunction with a greater abundance of pyruvate in the NpH group. This suggests that more PK could have produced more pyruvate. Conversely, some have determined that PK activity has a limited role in postmortem glycolysis (Allison et al., 2003; England et al., 2014). The analysis of increased pyruvate with decreased glycolytic capacity in the NpH group at 45 min, therefore, should be evaluated in conjunction with LDH and lactate abundances.

Lactate dehydrogenase catalyzes the reversible oxidation of pyruvate and NADH to lactate,  $\text{NAD}^+$ , and  $\text{H}^+$ . Pyruvate would otherwise be converted to acetyl coenzyme A and enter into the citric acid cycle within mitochondria. In living muscle, the rate at which lactate is produced is dependent on oxygen availability to the muscle, which can be used for aerobic metabolism, and energy demands that can vary depending on physical work (Westerblad et al., 2010). In muscle early postmortem (45 min), energy demands are high because the body is trying to maintain homeostasis, and oxygen may still be available but is no longer being transported to the muscle, leading to lactate accumulation. Some have identified a greater abundance of LDH in glycolytic muscle (Krischek et al., 2019) in addition to a greater activity of LDH in low-quality pork loin, which is defined by pH and WHC (Cho et al., 2016). In the current study, lactate abundance at 45 min postmortem corresponded to the low ultimate pH of the LpH group despite the greater abundance of L-LDH in the NpH group. The greater abundance of both L-LDH and PK in the NpH group can be partially explained by the greater concentration of pyruvate and the lesser concentration of lactate in the NpH group.

Altogether, these metabolic marker results indicate that a greater accumulation of lactate in the LpH group is most likely due to the extended postmortem enzymatic activity. As LDH consumes protons to reduce pyruvate to lactate, it buffers the system and delays  $\text{H}^+$  accumulation (Scheffler et al., 2011). This supports the current study finding that the LpH group can accumulate more lactate at 45 min postmortem with no differences in 45-min pH. Matarneh et al. (2015) have shown comparable results in the *longissimus lumborum* of pigs with the  $\text{AMPK}_{\gamma 3}^{\text{R200Q}}$  mutation. The  $\text{AMPK}_{\gamma 3}^{\text{R200Q}}$  mutation consistently causes low ultimate pH in fresh pork. Loins from these pigs had

similar lactate levels at 24 h postmortem as loins from wild-type pigs, whereas the wild-type pigs had higher ultimate pH (Matarneh et al., 2015). These researchers partly attributed this observation to an improved buffering capacity of the wild-type pigs, as defined by the change in NaOH per grams of tissue divided by the corresponding change in pH. Further, Matarneh et al. (2015) explained that net lactate from 0 to 24 h postmortem—in addition to buffering capacity—will determine the ultimate pH. Therefore,  $H^+$  are accumulated due to lactate production, but this measurement may not reflect pH, as shown in the current study. Lactate accumulation at 45 min postmortem only means that loins in the LpH group had the potential for lower ultimate pH throughout the conversion of muscle to meat. In other words, lactate measurements at a single time point (45 min postmortem) may not directly equate to lower pH at that time. The accumulation of lactate over time will result in lower pH values. This may explain the differences in pH observed in this study at 14 d postmortem but not 45 min, 3 h, or 6 h.

$\alpha$ -Actin was more abundant in the sarcoplasmic extract of meat from the NpH group. Notably,  $\alpha$ -actin would normally be found in the myofibrillar fraction rather than the sarcoplasmic fraction. Two explanations for this observation are (1) increased degradation of proteins early postmortem and (2) fewer actomyosin cross bridges were formed at 45 min postmortem. Actin solubility, therefore, has an association with the ultimate pH. Similar results have shown several soluble actin spots from pork loin negatively correlated with shear force (Lametsch et al., 2003). Skeletal muscle structure can significantly impact the stability and activity of several glycolytic enzymes (Roberts and Somero, 1987; Beitner, 1993; Ertbjerg and Puolanne, 2017). Therefore, the observation that actin solubility is linked to extended postmortem glycolysis may indicate mechanisms behind glycolytic protein activity in the early-postmortem period.

The accumulation of fructose 6-phosphate in the early-postmortem LpH group is an important observation. England et al. (2014) showed that PFK activity decreased with pH decline in an *in vitro* system and was no longer active below pH 5.5. Conversely, the current study shows that all of the LpH samples and several NpH samples were below pH 5.5 at 14 d postmortem. This means that some structures, such as filamentous actin (Roberts and Somero, 1987), can maintain PFK activity or that enough substrates are in the pipeline when pH reached 5.5.

A greater amount of substrate (fructose 6-phosphate) that can pass PFK will lead to more glycolytic flux and

low ultimate pH (England et al., 2014). In the current study, a significant accumulation of fructose 6-phosphate was observed in the LpH group despite western blots confirming that PFK abundance was similar at both 45 min and 14 d postmortem (Table 5). These results indicate that more fructose 6-phosphate could pass PFK at 45 min postmortem in the NpH group. One explanation may be that when pH is still high, the substrate can clear PFK more quickly in the NpH group. In other words, fructose 6-phosphate accumulation in the LpH group may have been due to structural restraint from myofibrils, identified by less soluble actin limiting the conversion of fructose 6-phosphate to fructose 1,6-bisphosphate. This structural restraint would help extend glycolysis in the LpH samples and enable a low pH at 14 d postmortem (Beitner, 1993; Ertbjerg and Puolanne, 2017).

Heat shock proteins play a dynamic role in early-postmortem metabolism, and, as discussed previously, they are associated with fresh pork quality traits such as tenderness (Ma and Kim, 2020). Soluble proteins in the NpH group had a greater abundance of HSP70 and  $\alpha 2$ -heat shock glycoprotein. These proteins are chaperones, meaning they assist in protein functional and structural maintenance (Ross et al., 2015). Heat shock protein 70 is reported to have antiapoptotic functions. Antiapoptotic proteins are closely associated with mitochondria (Picard et al., 2010; England et al., 2013). This could mean that increased HSP70 will enable the cell to handle stress like apoptosis and oxidation of mitochondria (Grubbs et al., 2014), resulting in higher-quality products.

A greater abundance of heat shock proteins in the sarcoplasm of the NpH group is in contradiction to other reports, identifying these stress-related proteins in lower-quality pork *longissimus thoracis* samples (Di Luca et al., 2013). Poleti et al. (2018) also reported a greater abundance of HSP70 in beef *longissimus thoracis* with normal pH classification (pH < 5.8) versus the high-pH classification (pH > 6.0). The current study showed more abundance of soluble HSP70 in the NpH group, resulting from differences in localization of early-postmortem proteins between the NpH and LpH groups.

Heat shock protein in the soluble fraction might indicate a greater abundance of mitochondria or disruption of mitochondria (Schulte et al., 2020). Furthermore, loins in the LpH group may have exhibited more effective antiapoptotic capabilities. This is because their mitochondria may have a closer association with myofibrils, thus altering mitochondrial function in the early-postmortem environment. This hypothesis

is supported by a study in mice that mitochondrial respiration decreases with less intermediate filament, linking mitochondria to the z-disk (Milner et al., 2000).

Alternatively, loins in the NpH group could simply have a greater abundance of these heat shock proteins that extend antiapoptotic activity in postmortem meat (Poletti et al., 2018). Under these conditions, pyruvate could be shuttled to functional mitochondria and be metabolized in the citric acid cycle. Metabolism of pyruvate would result in less total lactate production at 45 min in the NpH group.

Metabolite profile in muscle during the early-postmortem period can inform the dynamic changes in the conversion of muscle to meat. The current study identifies several glycolytic proteins that were all more abundant in the NpH group. This observation contradicts other reports that associate more glycolytic proteins with more glycolytic potential and lower-quality meat (Chauhan and England, 2018; Álvarez et al., 2019; Boudon et al., 2020). Therefore, glycolytic enzymes identified at 45 min postmortem should be analyzed individually to understand their relationship with pH decline and pork quality.

Fructose biphosphate aldolase catalyzes the conversion of fructose 1,6-bisphosphate into dihydroxyacetone phosphate and GAPDH. There was a greater extent of phosphorylation of ALDO in pork that demonstrated a rapid pH decline in a study by Huang et al. (2011). Maintained ALDO activity in the LpH group might be a result of phosphorylation. The greater abundance of ALDO in the NpH group of this study might be explained by less ALDO solubility in the LpH group. A complex of fructose 1,6-bisphosphate and ALDO around the z-disk may alter the signaling and activity of fructose 1,6-bisphosphate (Rakus et al., 2004). Therefore, a greater abundance of sarcoplasmic ALDO in the NpH loins may indicate variations in molecular complexes, causing glycolytic molecule signaling changes.

Glyceraldehyde 3-phosphate dehydrogenase catalyzes the conversion of glyceraldehyde 3-phosphate and  $\text{NAD}^+$  to 1,3 bisphosphoglycerate and NADH. Kim et al. (2019) identified a greater abundance of GAPDH in the medial region of the pork's *longissimus* muscle and concluded that GAPDH might contribute to color variations in pork loins. Moreover, several studies have revealed a greater abundance of GAPDH in glycolytic muscles (Damon et al., 2012; England et al., 2016). However, in the present study, it was shown that despite LpH samples having presumably higher glycolytic capacity, one spot of GAPDH was identified as more abundant in the NpH group of the 3–10 pH strip.

$\beta$ -enolase is the muscle-specific isoform of enolase, catalyzing the hydrolysis of 2-phosphoglycerate to phosphoenolpyruvate. A previous study has identified greater amounts of  $\beta$ -enolase in early-postmortem pork *longissimus* muscle samples with lower 24-h postmortem pH ( $\text{pH } 5.55 \pm 0.03$ ) and lower WHC (Subramaniyan et al., 2017). Those findings contradict the current results that showed more abundance of  $\beta$ -enolase in the NpH group. Clark et al. (2002) revealed that  $\beta$ -enolase could bind to the M-line, creating a glycolytic complex. Keller et al. (2000) identified  $\beta$ -enolase at the M-line and hypothesized that this localization might contribute to ATP production. Therefore, changes in this protein's solubility may be associated with variations in protein activity (Di Luca et al., 2013), meaning that this structure may maintain postmortem glycolytic metabolism and explain a lesser abundance of  $\beta$ -enolase in the soluble, sarcoplasmic fraction of LpH samples.

## Conclusions

The objective of this study was to determine the extent to which early-postmortem proteome and metabolome influence ultimate pH and pork loin quality. We found that subtle differences in day-14 pH were a good indicator of fresh pork loin quality. These results support the proposed hypothesis that small variations in ultimate pH result in differences in pork quality. Improved quality traits were supported by increased protein degradation in NpH on day 14. The results also support the proposed hypothesis that natural variations in glycolytic capacity are related to ultimate pH and are detectable in metabolomics and proteomic profiles at 45 min postmortem. Therefore, potential mechanisms behind less extreme variations in pH decline were identified. Peroxiredoxin-2 differences at 45 min postmortem may contribute to variation in oxidation (Joseph et al., 2012). This may explain the improved star probe, better color scores, and darker pork in the NpH group. Furthermore, heat shock proteins identified in the NpH group may reflect antiapoptotic functions, thus supporting postmortem activity of proteolytic enzymes or mitochondria, which could be related to proteolysis, tenderness, color development, and postmortem pH decline (Tang et al., 2005; Matarneh et al., 2018).

Proteomic results—in conjunction with metabolite abundances—create the following hypotheses for further investigation: (1) metabolic enzymes from early-postmortem samples bind to myofibrillar proteins,

resulting in lower protein solubility and maintained glycolytic activity of samples that ultimately results in LpH, and (2) passage of pyruvate to lactate may be related to soluble LDH, PK, and mitochondria function, which can play a significant role in glycolysis and pH decline, resulting in small yet significant variations in ultimate pH.

## Acknowledgments

Funding was provided by the United States Department of Agriculture National Institute of Food and Agriculture Award 2019-67017-29181, Iowa Agricultural and Home Economics Experiment Station project number 3721, and the National Pork Checkoff.

## Literature Cited

- Allison, C. P., R. O. Bates, A. M. Booren, R. C. Johnson, and M. E. Doumit. 2003. Pork quality variation is not explained by glycolytic enzyme capacity. *Meat Sci.* 63:17–22. [https://doi.org/10.1016/s0309-1740\(02\)00046-3](https://doi.org/10.1016/s0309-1740(02)00046-3).
- Álvarez, C., L. Morán, D. F. Keenan, A.-M. Mullen, and G. Delgado-Pando. 2019. Mechanical and biochemical methods for rigor measurement: Relationship with eating quality. *J. Food Quality.* 2019:1–13. <https://doi.org/10.1155/2019/1894543>.
- Bee, G., A. L. Anderson, S. M. Lonergan, and E. Huff-Lonergan. 2007. Rate and extent of pH decline affect proteolysis of cytoskeletal proteins and water-holding capacity in pork. *Meat Sci.* 76:359–365. <https://doi.org/10.1016/j.meatsci.2006.12.004>.
- Beitner, R. 1993. Control of glycolytic enzymes through binding to cell structures and by glucose-1, 6-bisphosphate under different conditions. The role of Ca<sup>2+</sup> and calmodulin. *Int. J. Biochem.* 25:297–305. [https://doi.org/10.1016/0020-711X\(93\)90616-M](https://doi.org/10.1016/0020-711X(93)90616-M).
- Boudon, S., D. Ounaissi, D. Viala, V. Monteils, B. Picard, and I. Cassar-Malek. 2020. Label free shotgun proteomics for the identification of protein biomarkers for beef tenderness in muscle and plasma of heifers. *J. Proteomics.* 217:103685. <https://doi.org/10.1016/j.jprot.2020.103685>.
- Brewer, M. S., L. G. Zhu, and F. K. McKeith. 2001. Marbling effects on quality characteristics of pork loin chops: Consumer purchase intent, visual and sensory characteristics. *Meat Sci.* 59:153–163. [https://doi.org/10.1016/S0309-1740\(01\)00065-1](https://doi.org/10.1016/S0309-1740(01)00065-1).
- Carlson, K. B., K. J. Prusa, C. A. Fedler, E. M. Steadham, E. Huff-Lonergan, and S. M. Lonergan. 2017. Proteomic features linked to tenderness of aged pork loins. *J. Anim. Sci.* 95:2533–2546. <https://doi.org/10.2527/jas.2016.1122>.
- Chauhan, S. S., and E. M. England. 2018. Postmortem glycolysis and glycogenolysis: Insights from species comparisons. *Meat Sci.* 144:118–126. <https://doi.org/10.1016/j.meatsci.2018.06.021>.
- Cho, J. H., R. H. Lee, Y.-J. Jeon, S.-M. Park, J.-C. Shin, S.-H. Kim, J. Y. Jeong, H.-S. Kang, N.-J. Choi, K. S. Seo, Y. S. Cho, M. S. S. Kim, S. Ko, J.-M. Seo, S.-Y. Lee, J.-H. Shim, and J.-I. Chae. 2016. Proteomic assessment of the relevant factors affecting pork meat quality associated with Longissimus dorsi muscles in Duroc pigs. *Asian Austral. J. Anim.* 29:1653–1663. <https://doi.org/10.5713/ajas.16.0050>.
- Chong, J., O. Soufan, C. Li, I. Caraus, S. Li, G. Bourque, D. S. Wishart, and J. Xia. 2018. MetaboAnalyst 4.0: Towards more transparent and integrative metabolomics analysis. *Nucleic Acids Res.* 46:W486–W494. <https://doi.org/10.1093/nar/gky310>.
- Clark, K. A., A. S. McElhinny, M. C. Beckerle, and C. C. Gregorio. 2002. Striated muscle cytoarchitecture: An intricate web of form and function. *Annu. Rev. Cell Dev. Bi.* 18:637–706. <https://doi.org/10.1146/annurev.cellbio.18.012502.105840>.
- Damon, M., J. Wyszynska-Koko, A. Vincent, F. Héroult, and B. Lebret. 2012. Comparison of muscle transcriptome between pigs with divergent meat quality phenotypes identifies genes related to muscle metabolism and structure. *PLOS ONE.* 7: e33763. <https://doi.org/10.1371/journal.pone.0033763>.
- Di Luca, A., G. Elia, R. Hamill, and A. M. Mullen. 2013. 2D DIGE proteomic analysis of early post mortem muscle exudate highlights the importance of the stress response for improved water-holding capacity of fresh pork meat. *Proteomics.* 13:1528–1544. <https://doi.org/10.1002/pmic.201200145>.
- England, E. M., S. K. Matarneh, E. M. Oliver, A. Apaoblaza, T. L. Scheffler, H. Shi, and D. E. Gerrard. 2016. Excess glycogen does not resolve high ultimate pH of oxidative muscle. *Meat Sci.* 114:95–102. <https://doi.org/10.1016/j.meatsci.2015.10.010>.
- England, E. M., S. K. Matarneh, T. L. Scheffler, C. Wacht, and D. E. Gerrard. 2014. pH inactivation of phosphofructokinase arrests postmortem glycolysis. *Meat Sci.* 98:850–857. <https://doi.org/10.1016/j.meatsci.2014.07.019>.
- England, E. M., S. K. Matarneh, T. L. Scheffler, C. Wacht, and D. E. Gerrard. 2015. Altered AMP deaminase activity may extend postmortem glycolysis. *Meat Sci.* 102:8–14. <https://doi.org/10.1016/j.meatsci.2014.11.009>.
- England, E. M., T. L. Scheffler, S. C. Kasten, S. K. Matarneh, and D. E. Gerrard. 2013. Exploring the unknowns involved in the transformation of muscle to meat. *Meat Sci.* 95:837–843. <https://doi.org/10.1016/j.meatsci.2013.04.031>.
- Ertbjerg, P., and E. Puolanne. 2017. Muscle structure, sarcomere length and influences on meat quality: A review. *Meat Sci.* 132:139–152. <https://doi.org/10.1016/j.meatsci.2017.04.261>.
- Font-i-Furnols, M., and L. Guerrero. 2014. Consumer preference, behavior and perception about meat and meat products: An overview. *Meat Sci.* 98:361–371. <https://doi.org/10.1016/j.meatsci.2014.06.025>.
- Grubbs, J. K., E. Huff-Lonergan, N. K. Gabler, J. C. M. Dekkers, and S. M. Lonergan. 2014. Liver and skeletal muscle mitochondria proteomes are altered in pigs divergently selected for residual feed intake. *J. Anim. Sci.* 92:1995–2007. <https://doi.org/10.2527/jas.2013-7391>.
- Henckel, P., A. Karlsson, M. T. Jensen, N. Oksbjerg, and J. S. Petersen. 2002. Metabolic conditions in Porcine longissimus muscle immediately pre-slaughter and its influence on peri- and post mortem energy metabolism. *Meat Sci.* 62:145–155. [https://doi.org/10.1016/S0309-1740\(01\)00239-X](https://doi.org/10.1016/S0309-1740(01)00239-X).

- Honegger, L. T., E. Richardson, E. D. Schunke, A. C. Dilger, and D. D. Boler. 2019. Final internal cooking temperature of pork chops influenced consumer eating experience more than visual color and marbling or ultimate pH. *J. Anim. Sci.* 97:2460–2467. <https://doi.org/10.1093/jas/skz117>.
- Huang, H., M. R. Larsen, A. H. Karlsson, L. Pomponio, L. N. Costa, and R. Lametsch. 2011. Gel-based phosphoproteomics analysis of sarcoplasmic proteins in postmortem porcine muscle with pH decline rate and time differences. *Proteomics*. 11:4063–4076. <https://doi.org/10.1002/pmic.201100173>.
- Huff-Loneragan, E., T. J. Baas, M. Malek, J. C. M. Dekkers, K. Prusa, and M. F. Rothschild. 2002. Correlations among selected pork quality traits. *J. Anim. Sci.* 80:617–627. <https://doi.org/10.2527/2002.803617x>.
- Huff-Loneragan, E., and S. M. Lonergan. 2005. Mechanisms of water-holding capacity of meat: The role of postmortem biochemical and structural changes. *Meat Sci.* 71:194–204. <https://doi.org/10.1016/j.meatsci.2005.04.022>.
- Huff-Loneragan, E., W. Zhang, and S. M. Lonergan. 2010. Biochemistry of postmortem muscle — Lessons on mechanisms of meat tenderization. *Meat Sci.* 86:184–195. <https://doi.org/10.1016/j.meatsci.2010.05.004>.
- Hughes, J. M., S. K. Oiseth, P. P. Purslow, and R. D. Warner. 2014. A structural approach to understanding the interactions between colour, water-holding capacity and tenderness. *Meat Sci.* 98:520–532. <https://doi.org/10.1016/j.meatsci.2014.05.022>.
- Joseph, P., S. P. Suman, G. Rentfrow, S. Li, and C. M. Beach. 2012. Proteomics of muscle-specific beef color stability. *J. Agr. Food Chem.* 60:3196–3203. <https://doi.org/10.1021/jf204188v>.
- Kastenschmidt, L. L., W. G. Hoekstra, and E. J. Briskey. 1968. Glycolytic intermediates and co-factors in “fast-” and “slow-glycolyzing” muscles of the pig. *J. Food Sci.* 33:151–158. <https://doi.org/10.1111/j.1365-2621.1968.tb01341.x>.
- Keller, A., J. Demeurie, T. Merkulova, G. Géraud, C. Cywiner-Golenzer, M. Lucas, and F.-P. Châtelet. 2000. Fibre-type distribution and subcellular localisation of  $\alpha$  and  $\beta$  enolase in mouse striated muscle. *Biol. Cell.* 92:527–535. [https://doi.org/10.1016/S0248-4900\(00\)01103-5](https://doi.org/10.1016/S0248-4900(00)01103-5).
- Kim, G.-D., J.-Y. Jeong, H.-S. Yang, and S. J. Hur. 2019. Differential abundance of proteome associated with intramuscular variation of meat quality in porcine longissimus thoracis et lumborum muscle. *Meat Sci.* 149:85–95. <https://doi.org/10.1016/j.meatsci.2018.11.012>.
- Krischek, C., J. Popp, and A. R. Sharifi. 2019. Biochemical alterations in the Musculus triceps brachii and Musculus longissimus thoracis during early postmortem period in pigs. *Meat Sci.* 152:121–126. <https://doi.org/10.1016/j.meatsci.2019.02.023>.
- Lametsch, R., A. Karlsson, K. Rosenvold, H. J. Andersen, P. Roepstorff, and E. Bendixen. 2003. Postmortem proteome changes of porcine muscle related to tenderness. *J. Agr. Food Chem.* 51:6992–6997. <https://doi.org/10.1021/jf034083p>.
- Lomiwes, D., M. M. Farouk, E. Wiklund, and O. A. Young. 2014. Small heat shock proteins and their role in meat tenderness: A review. *Meat Sci.* 96:26–40. <https://doi.org/10.1016/j.meatsci.2013.06.008>.
- Lowry, O. H., N. J. Rosebrough, A. L. Farr, and R. J. Randall. 1951. Protein measurement with the Folin phenol reagent. *J. Biol. Chem.* 193:265–275.
- Lusk, J. L., G. T. Tonsor, T. C. Schroeder, and D. J. Hayes. 2018. Effect of government quality grade labels on consumer demand for pork chops in the short and long run. *Food Policy.* 77:91–102. <https://doi.org/10.1016/j.foodpol.2018.04.011>.
- Ma, D., and Y. H. B. Kim. 2020. Proteolytic changes of myofibrillar and small heat shock proteins in different bovine muscles during aging: Their relevance to tenderness and water-holding capacity. *Meat Sci.* 163:108090. <https://doi.org/10.1016/j.meatsci.2020.108090>.
- Maddock Carlin, K. R., E. Huff-Loneragan, L. J. Rowe, and S. M. Lonergan. 2006. Effect of oxidation, pH, and ionic strength on calpastatin inhibition of  $\mu$ - and m-calpain. *J. Anim. Sci.* 84:925–937. <https://doi.org/10.2527/2006.844925x>.
- Mancini, R. A., and M. C. Hunt. 2005. Current research in meat color. *Meat Sci.* 71:100–121. <https://doi.org/10.1016/j.meatsci.2005.03.003>.
- Matarneh, S. K., M. Beline, S. de Luz e Silva, H. Shi, and D. E. Gerrard. 2018. Mitochondrial F<sub>1</sub>-ATPase extends glycolysis and pH decline in an in vitro model. *Meat Sci.* 137:85–91. <https://doi.org/10.1016/j.meatsci.2017.11.009>.
- Matarneh, S. K., E. M. England, T. L. Scheffler, and D. E. Gerrard. 2017a. The conversion of muscle to meat. In: F. Toldra, editor, *Lawrie’s Meat Science*. 8th ed. Woodhead Publishing, Cambridge, UK. p. 159–185.
- Matarneh, S. K., E. M. England, T. L. Scheffler, E. M. Oliver, and D. E. Gerrard. 2015. Net lactate accumulation and low buffering capacity explain low ultimate pH in the longissimus lumborum of AMPK $\gamma$ 3<sup>R200Q</sup> mutant pigs. *Meat Sci.* 110:189–195. <https://doi.org/10.1016/j.meatsci.2015.07.023>.
- Matarneh, S. K., E. M. England, T. L. Scheffler, C.-N. Yen, J. C. Wicks, H. Shi, and D. E. Gerrard. 2017b. A mitochondrial protein increases glycolytic flux. *Meat Sci.* 133:119–125. <https://doi.org/10.1016/j.meatsci.2017.06.007>.
- Milner, D. J., M. Mavroidis, N. Weisleder, and Y. Capetanaki. 2000. Desmin cytoskeleton linked to muscle mitochondrial distribution and respiratory function. *J. Cell Biol.* 150:1283–1298. <http://doi.org/10.1083/jcb.150.6.1283>.
- Mookerjee, S. A., D. G. Nicholls, and M. D. Brand. 2016. Determining maximum glycolytic capacity using extracellular flux measurements. *PLOS ONE*. 11:e0152016. <https://doi.org/10.1371/journal.pone.0152016>.
- Morzel, M., P. Gatellier, T. Sayd, M. Renerre, and E. Laville. 2006. Chemical oxidation decreases proteolytic susceptibility of skeletal muscle myofibrillar proteins. *Meat Sci.* 73:536–543. <https://doi.org/10.1016/j.meatsci.2006.02.005>.
- NPPC. 2000. Pork composition and quality assessment procedures. National Pork Producers Council, Washington, DC.
- Ohlendieck, K. 2010. Proteomics of skeletal muscle glycolysis. *BBA-Proteins Proteom.* 1804:2089–2101. <https://doi.org/10.1016/j.bbapap.2010.08.001>.
- Outhouse, A. C., E. T. Helm, B. M. Patterson, J. C. M. Dekkers, W. M. Rauw, K. J. Schwartz, N. K. Gabler, E. Huff-Loneragan,

- and S. M. Lonergan. 2019. Effect of a dual enteric and respiratory pathogen challenge on swine growth, efficiency, carcass composition, and pork quality. *J. Anim. Sci.* 97:4710–4720. <https://doi.org/10.1093/jas/skz332>.
- Picard, B., C. Berri, L. Lefaucheur, C. Molette, T. Sayd, and C. Terlouw. 2010. Skeletal muscle proteomics in livestock production. *Brief. Funct. Genomics.* 9:259–278. <https://doi.org/10.1093/bfpg/elq005>.
- Picard, B., and M. Gagaoua. 2020. Meta-proteomics for the discovery of protein biomarkers of beef tenderness: An overview of integrated studies. *Food Res. Int.* 127:1–23. <https://doi.org/10.1016/j.foodres.2019.108739>.
- Picard, B., M. Gagaoua, D. Micol, I. Cassar-Malek, J. F. Hocquette, and C. E. M. Terlouw. 2014. Inverse relationships between biomarkers and beef tenderness according to contractile and metabolic properties of the muscle. *J. Agr. Food Chem.* 62:9808–9818. <https://doi.org/10.1021/jf501528s>.
- Poleti, M. D., C. T. Moncau, B. Silva-Vignato, A. F. Rosa, A. R. Lobo, T. R. Cataldi, J. A. Negrão, S. L. Silva, J. P. Eler, and J. C. d. C. Balieiro. 2018. Label-free quantitative proteomic analysis reveals muscle contraction and metabolism proteins linked to ultimate pH in bovine skeletal muscle. *Meat Sci.* 145:209–219. <http://doi.org/10.1016/j.meatsci.2018.06.041>.
- Rakus, D., M. Pasek, H. Krotkiewski, and A. Dzugaj. 2004. Interaction between muscle aldolase and muscle fructose 1, 6-bisphosphatase results in the substrate channeling. *Biochemistry.* 43:14948–14957. <https://doi.org/10.1021/bi048886x>.
- Richardson, E. L., B. Fields, A. C. Dilger, and D. D. Boler. 2018. The effects of ultimate pH and color on sensory traits of pork loin chops cooked to a medium-rare degree of doneness. *J. Anim. Sci.* 96:3768–3776. <https://doi.org/10.1093/jas/sky258>.
- Roberts, S. J., and G. N. Somero. 1987. Binding of phosphofructokinase to filamentous actin. *Biochemistry.* 26:3437–3442. <https://doi.org/10.1021/bi00386a028>.
- Ross, J. W., B. J. Hale, N. K. Gabler, R. P. Rhoads, A. F. Keating, and L. H. Baumgard. 2015. Physiological consequences of heat stress in pigs. *Anim. Prod. Sci.* 55:1381–1390. <https://doi.org/10.1071/an15267>.
- Scheffler, T. L., and D. E. Gerrard. 2007. Mechanisms controlling pork quality development: The biochemistry controlling post-mortem energy metabolism. *Meat Sci.* 77:7–16. <https://doi.org/10.1016/j.meatsci.2007.04.024>.
- Scheffler, T. L., S. Park, and D. E. Gerrard. 2011. Lessons to learn about postmortem metabolism using the AMPK $\gamma$ 3<sup>R200Q</sup> mutation in the pig. *Meat Sci.* 89:244–250. <https://doi.org/10.1016/j.meatsci.2011.04.030>.
- Schiaffino, S., and C. Reggiani. 1996. Molecular diversity of myofibrillar proteins: Gene regulation and functional significance. *Physiol. Rev.* 76:371–423. <https://doi.org/10.1152/physrev.1996.76.2.371>.
- Schulte, M. D., L. G. Johnson, E. A. Zuber, B. M. Patterson, A. C. Outhouse, C. A. Fedler, E. M. Steadham, D. A. King, K. J. Prusa, E. Huff-Lonergan, and S. M. Lonergan. 2019. Influence of postmortem aging and post-aging freezing on pork loin quality attributes. *Meat Muscle Biol.* 3:313–323. <https://doi.org/10.22175/mmb2019.05.0015>.
- Schulte, M. D., L. G. Johnson, E. A. Zuber, E. M. Steadham, D. A. King, E. J. Huff-Lonergan, and S. M. Lonergan. 2020. Investigation of the sarcoplasmic proteome contribution to the development of pork loin tenderness. *Meat Muscle Biol.* 4:1–14. <https://doi.org/10.22175/mmb.9566>.
- Schwägele, F., C. Haschke, K. O. Honikel, and G. Krauss. 1996. Enzymological investigations on the causes for the PSE-syndrome, I. Comparative studies on pyruvate kinase from PSE- and normal pig muscles. *Meat Sci.* 44:27–40. [https://doi.org/10.1016/s0309-1740\(96\)00046-0](https://doi.org/10.1016/s0309-1740(96)00046-0).
- Subramaniyan, S. A., D. R. Kang, Y. C. Jung, J. H. Jung, Y. I. Choi, M. J. Lee, H. S. Choe, and K. S. Shim. 2017. Comparative studies of meat quality traits and the proteome profile between low- and high-pH muscles in longissimus dorsi of Berkshire. *Can. J. Anim. Sci.* 97:640–649. <https://doi.org/10.1139/cjas-2016-0230>.
- Tang, J., C. Faustman, T. A. Hoagland, R. A. Mancini, M. Seyfert, and M. C. Hunt. 2005. Postmortem oxygen consumption by mitochondria and its effects on myoglobin form and stability. *J. Agr. Food Chem.* 53:1223–1230. <https://doi.org/10.1021/jf048646o>.
- Tarczyński, K., H. Siczowska, A. Zybert, E. Krzycio-Nieczyporuk, and K. Antosik. 2018. pH measured 24 hours post mortem should not be regarded as ultimate pH in pork meat quality evaluation. *S. Afr. J. Anim. Sci.* 48:1009–1016. <https://doi.org/10.4314/sajas.v48i6.2>.
- NIST. 2017. NIST Tandem Mass Spectral Library, 2017 Release. US Department of Commerce, National Institute of Standards and Technology. <http://chemdata.nist.gov/mass-spc/msms-search/>. (Accessed 13 November 2019).
- Wang, Y., R. Liu, Q. Hou, X. Tian, X. Fan, W. Zhang, and G. Zhou. 2020. Comparison of activity, expression and S-nitrosylation of glycolytic enzymes between pale, soft and exudative and red, firm and non-exudative pork during post-mortem aging. *Food Chem.* 314:126203. <https://doi.org/10.1016/j.foodchem.2020.126203>.
- Westerblad, H., J. D. Bruton, and A. Katz. 2010. Skeletal muscle: Energy metabolism, fiber types, fatigue, and adaptability. *Exp. Cell Res.* 316:3093–3099. <https://doi.org/10.1016/j.yexcr.2010.05.019>.

## Supplemental Table 1

Metabolites were identified from pork *longissimus thoracis et lumborum* samples using GC-MS. The abundance of each polar metabolite was normalized with moles of ribitol (0.0098  $\mu\text{mol}$ ), and nonpolar metabolites were normalized with moles of nonadecanoic fatty acid (0.005  $\mu\text{mol}$ ). The National Institutes of Standards and Technology mass spectral library (NIST, 2017) served as references for metabolites identified using the total ion mass spectrum. pH classifications were between d 14 postmortem pH classified as normal pH (pH, =5.59, 5.53-5.67) and low pH (pH, =5.42, 5.38-5.45). Fold change is shown as NpH/LpH.

	Fold Change	P-value
Polar		
N,O-Bistert-butyltrimethylsilylcarbamate	1.92	0.03
Glycolic acid	2.35	0.04
1,2-ethanediamine, N1-2-bis(trimethylsilylaminoethyl)-N1,N2,N2-tris(trimethylsilyl)	1.31	0.04
Ethanimidic acid	1.28	0.04
Phosphoric acid	1.73	0.05
Phosphoric acid, 2-isothiocyanatoethyl bis(trimethylsilyl) ester	0.52	0.05
Adenine	1.61	0.05
Glycerol 1-phosphate	1.16	0.05
L-glutamine	0.62	0.05
Glycerol-2-phosphate, phosphoric acid, 2-trimethylsiloxy-1-trimethylsilyloxymethylethyl bis(trimethylsilyl) ester	1.31	0.06
1,2,3,4,5,6-hexamethylcyclohexane	1.57	0.07
D-fructose, 1,3,4,5,6-pentakis-O-trimethylsilyl-, O-methylxime	0.79	0.08
Myo-inositol	1.28	0.09
Non-Polar		
9,12-octadecadienoic acid	1.12	0.03
Arachidonic acid	1.39	0.12